A Sunyaev-Zel'dovich Effect Survey for High Redshift Clusters

J.J. Mohr[1,4], J.E. Carlstrom[1], G.P. Holder[1], W.L. Holzapfel[2], M.K. Joy[3], E.M. Leitch[1], and E.D. Reese[1]

[1] University of Chicago, Chicago, IL USA
[2] University of California at Berkeley, Berkeley, CA USA
[3] NASA/Marshall Space Flight Center, Huntsville, AL, USA

to appear in the proceedings of the VLT Opening Symposium

Abstract. Interferometric observations of the Sunyaev-Zel'dovich Effect (SZE) toward clusters of galaxies provide sensitive cosmological probes. We present results from 1 cm observations (at BIMA and OVRO) of a large, intermediate redshift cluster sample. In addition, we describe a proposed, higher sensitivity array which will enable us to survey large portions of the sky. Simulated observations indicate that we will be able to survey one square degree of sky per month to sufficient depth that we will detect all galaxy clusters more massive than $2 \times 10^{14} h_{50}^{-1}\, M_\odot$, regardless of their redshift. We describe the cluster yield and resulting cosmological constraints from such a survey.

1 Interferometric Sunyaev-Zel'dovich Effect Imaging

Interactions between cosmic microwave background (CMB) photons and the hot, ionized plasma in galaxy clusters introduce changes in the spectrum of the CMB. At wavelengths of 1 cm we observe this Sunyaev-Zel'dovich Effect (SZE) [1] as a decrease in the intensity of the CMB; this decrement $\Delta T(R)$ at projected cluster radius R can be expressed as

$$\frac{\Delta T(R)}{T_{CMB}} = -2\frac{\sigma_T}{m_e c^2}\int dl\, n_e(l,R) k_B T_e(l,R) \tag{1}$$

where σ_T is the Thomson cross section, $m_e c^2$ is the electron rest mass, n_e is the electron number density and k_B is the Boltzmann constant. Note that the fractional change in the CMB temperature $\Delta T/T_{CMB}$ is independent of redshift; it depends only on properties of the ICM. Higher order corrections to this expression and a consideration of the effects of cluster peculiar velocities on the CMB spectrum can be found elsewhere (e.g., [2]).

The typical central decrement for a massive $\sim 10^{15}\ M_\odot$ galaxy cluster is ~ 1 mK, and for typical radio telescope system temperatures the SZE decrement is only a few parts in 10^5 of the power detected by the receiver, making SZE observations challenging. Characteristics of radio interferometry

[4] Chandra Fellow

make it well suited to meet this challenge. Perhaps the most important of these is that only the correlated portion of the receiver output is signal, while the uncorrelated output serves as noise; differential ground spillover and detector noise are naturally separated from the cluster decrement. Another is that interferometry effectively simultaneously differences over the sky, easily filtering the smoothly distributed $\sim$3 K background from the cluster SZE decrement we seek. Finally, with interferometry one obtains information on many scales simultaneously; by placing some dishes at larger separations it is straightforward to filter out point source contributions.

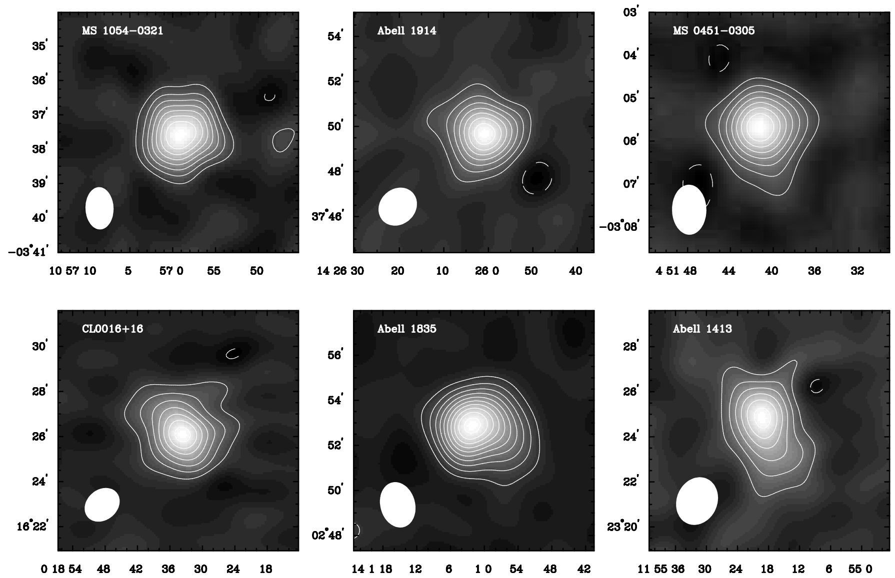

Fig. 1. SZE decrement images of six of the 27 clusters observed with the Sunyaev-Zel'dovich Imaging Experiment at BIMA and OVRO. Contours are spaced by 2σ, and the synthesized beam is represented by the white ellipse in the lower left of each frame.

Over the past several years, Carlstrom, Joy and collaborators have developed sensitive, low noise receivers and used them at the BIMA and OVRO observatories to obtain high quality SZE data on a sample of 27 intermediate redshift clusters [3]. Figure 1 contains greyscale SZE images and signal to noise contour overlays of 6 clusters. The contours are spaced by 2σ, and the white ellipses in the lower left of each frame represent the FWHM of the synthesized beam.

As demonstrated by Figure 1, the interferometric SZE Imaging Experiment does deliver high signal to noise SZE images of intermediate redshift clusters. We use these SZE data to constrain the cluster ICM distribution, and, in combination with published measurements of the ICM temperature, these data enable estimates of cluster ICM masses and mass fractions [4,5].

In combination with X-ray images of galaxy clusters, the SZE data allow one to estimate cluster sizes and measure direct, distance-ladder-independent distances. The X-ray surface brightness $I(R)$ at projected cluster radius R can be expressed as

$$I_X(R) = \frac{1}{4\pi(1+z)^4}\frac{\mu_e}{\mu_H}\int dl\, n_e^2(l,R)\Lambda(T_e) \tag{2}$$

where n_e is the electron number density, $\Lambda(T_e)$ is the temperature dependent cooling coefficient and $n_e = \rho/m_p\mu_e$. Note that $I(R)$ depends on the square of the electron density, and is highly redshift dependent. Because of the different dependence on the electron density, observations of $I(R)$ and $\Delta T/T_{CMB}$ provide a direct measure of the line of sight distance through the cluster. With additional assumptions about the cluster geometry, we can combine this line of sight size with the angular size of the cluster on the sky to estimate the cluster angular diameter distance D_A. We are currently using archival X-ray data to finalize distance estimates in our ensemble of 27 SZE clusters [6].

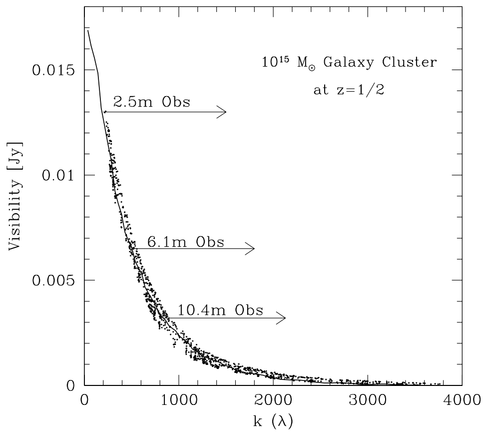

Fig. 2. One advantage of 2.5 m telescopes over the currently available 6.1 m BIMA and 10 m OVRO dishes is clear in this plot of cluster visibility versus k which is the telescope separation in units of the observing wavelength (1 cm). The cluster visibility falls off exponentially with k, yielding significant gains for smaller telescopes which can sample the visibility at smaller separations. The points are visibilities from a simulated galaxy cluster, and the line is the best fit model.

2 The Proposed SZE Interferometric Array

The difficulty of detecting X-ray emission from high redshift clusters– even with the high quality X-ray instruments available today– is made clear by Eqn. 2. Indeed, it is the redshift independent nature of the SZE (see Eqn. 1) that makes it an ideal tool for studying collapsed structures at high redshift. The current best instruments for SZE studies of high redshift clusters do not have the sensitivity required to detect sizeable numbers of clusters in a non-targeted search within reasonable observing times of 1 mth to 1 yr. Therefore, we have proposed to build a new array composed of ten 2.5 m dishes and a wide-band digital correlator. This array, when operating at 1 cm, is optimized for high redshift cluster detection and will be approximately 100 times more sensitive than our current SZE Imaging Experiment on BIMA.

In this era of large telescopes it may be surprising to learn that the best telescope size for SZE cluster studies is 2.5 m. There are two main reasons for this. First, the angular size θ_{BEAM} of the primary beam of a radio telescope scales with the dish diameter D as $\theta_{BEAM} \propto \lambda_{obs}/D$, where λ_{obs} is the observation wavelength. θ_{BEAM} determines the field size in a survey, and cluster signal on scales larger than $\theta_{BEAM}/2$ is lost. For 1 cm observations on a 6.1 m dish, the FWHM of the primary beam is $\theta_{BEAM} \sim 6$ arcmin, whereas for the 2.5 m telescopes $\theta_{BEAM} \sim 15$ arcmin. The primary beam of a 2.5 m dish is better matched to cluster angular scales than a 6.1 m dish. Second, as is shown graphically in Figure 2, interferometry samples the cluster visibility, which is the Fourier transform of the CMB decrement distribution on the sky. Cluster visibilities typically fall off exponentially with distance from the origin k (as opposed to point sources whose Fourier transforms are independent of k). Therefore, with smaller dishes one samples a region of the U-V plane where there is significantly more cluster flux.

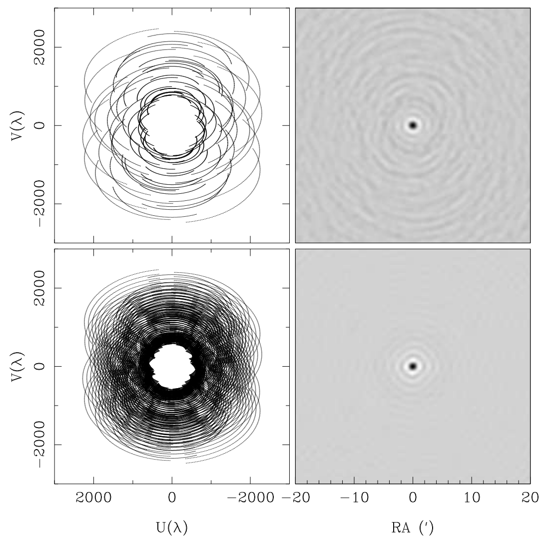

Fig. 3. The wide-band correlator allows us to take advantage of a larger portion of the signal output by the 10 GHz bandwidth receivers. This translates into higher sensitivity and more coverage in the U-V plane. The left panels show the U-V coverage for a 7 hr observation with the current correlator (upper) and the proposed correlator (lower). The right panels show the synthesized beam for each observation. The coverage available with the new correlator leads to lower sidelobes in the synthesized beam and enhanced image quality.

The proposed wide-band digital correlator will enable us to use a larger fraction of the signal output from the 10 GHz bandwidth receivers. Currently, the maximum bandwidth at BIMA is ∼800 MHz; thus, the proposed 8 GHz correlator will increase the sensitivity by an order of magnitude. In addition to higher throughput, the wide-band correlator provides enhanced image quality. As is apparent in Figure 3, the fraction of the U-V plane sampled in a 7 hr exposure with the old correlator (top left) is much smaller than the fraction sampled in the same exposure with the new correlator (bottom left). This additional U-V coverage leads to a synthesized beam (right panels) which has smaller sidelobes. This enhanced image quality simplifies structure detection in SZE images.

3 The SZE Galaxy Cluster Survey

X-ray samples of high redshift clusters are disappointingly small, primarily because of the strong redshift dependence of cluster emission (see Eqn. 2); only the most luminous clusters at each redshift tend to be found. However, with this sensitive new SZE array, we will be able to carry out a survey of ~ 1 deg^2 per month and detect all clusters more massive than $2\times10^{14}h_{50}^{-1}\ M_\odot$, independent of their redshift. Interestingly, the cluster selection function from such a survey is essentially a cut in cluster binding mass. So not only will an SZE survey yield a sizeable high redshift cluster sample for the first time, but the survey will also deliver a sample which is much easier to understand than typical X-ray samples at intermediate redshift.

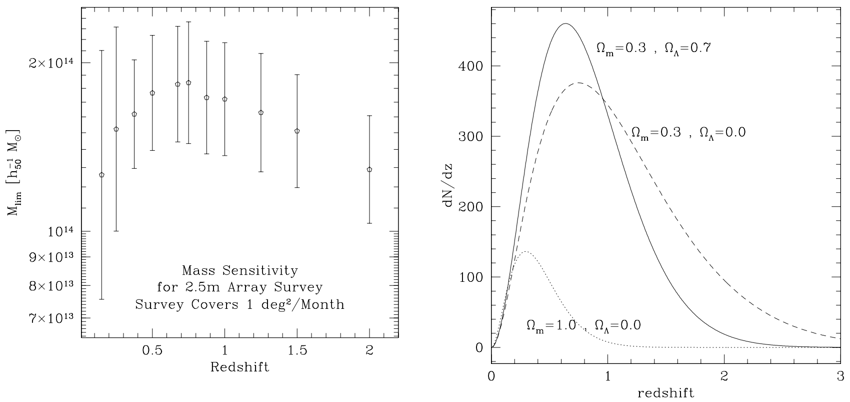

Fig. 4. The limiting mass M_{lim} of our proposed SZE survey versus redshift (left). We expect to detect all clusters more massive than $2\times10^{14}h_{50}^{-1}\ M_\odot$, independent of their redshift! To the right we plot the abundance of clusters more massive than M_{lim} as a function of redshift. These Press-Schechter models are normalized to produce the observed cluster abundance in the nearby universe.

We determine the survey mass limit as a function of redshift through mock observations of N-body plus SPH simulations of galaxy clusters. These mock SZE observations include noise and have exposures tuned so that we will be able to survey 1 deg^2 in a month. The N-body plus SPH simulations are state of the art simulations sampled from four different cosmological models: (1) SCDM: standard, biased $\Omega = 1$ CDM, (2) OCDM: unbiased $\Omega_m = 0.3$ CDM, (3) LCDM: unbiased $\Omega_m = 0.3$ and $\Omega_\lambda = 0.7$ CDM, and (4) τCDM:

$\Omega_m = 1$ but CDM power spectrum with $\Gamma = 0.24$ (see [7,8] for more details). These simulations include only gas dynamics and gravity. We use three particle species; this allows us to follow tidal fields from surrounding large scale structure while still resolving the dynamics in the cluster core. We incorporate no early heating of the ICM from galaxy formation.

To determine the detection limit at each redshift we use outputs of the 48 simulations from the appropriate redshift; with this approach the morphological evolution of galaxy clusters is naturally included. We determine the detection probability in each mock observation by fitting a cluster model and determining the $\Delta\chi^2$ between the best fitting and null models. We set our detection threshold at 5σ.

Figure 4 (left) is a plot of limiting mass versus redshift. The uncertainties on the limiting mass correspond to the scatter about the best fit $\Delta\chi^2$-binding mass relation, determined using mock observations of the entire cluster ensemble at each redshift; this scatter is an indication of the morphological sensitivity of the detection threshold. We find that the limiting mass is independent of cosmological model– at least for the four models tested. Also in Figure 4 (right) is a Press-Schechter estimate of the surface density of clusters more massive than $M_{lim} = 2 \times 10^{14} h_{50}^{-1}\ M_\odot$ as a function of redshift for three cosmological models (noted on the figure). These models are all normalized to produce the correct cluster abundance at the present epoch. Note the cosmological sensitivity of the cluster surface densities; we expect to find very few clusters with our survey if $\Omega = 1$, whereas for more favored, low Ω_0 models we expect hundreds of clusters [10].

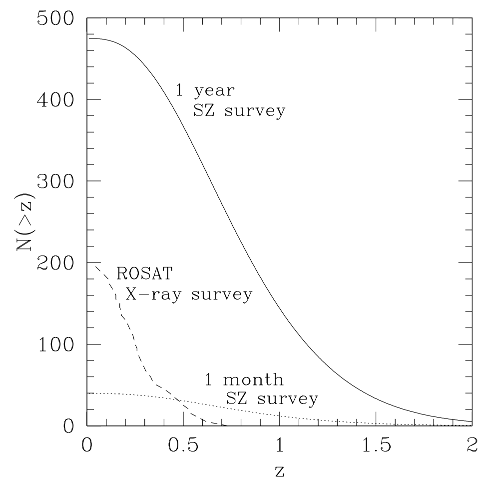

Fig. 5. We plot the expected yield of our proposed SZE survey after one month (dotted) and one year (solid) if $\Omega_0 = 0.3$ and $\Omega_\lambda = 0.7$. For comparison we plot the yield of the ROSAT PSPC deep cluster survey (dashed). After one month we will have more clusters at redshift $z > 0.5$ than the entire ROSAT survey. After one year we will have ∼100 clusters at redshifts $z > 1$ and ∼400 clusters at redshifts $z.0.5$.

In Figure 5 we plot the survey yield after one month (dotted line) and one year (solid line), where we have assumed that the currently favored model $\Omega_m = 0.3$ and $\Omega_\lambda = 0.7$ is correct (if $\Omega_\lambda = 0$ the cluster count increases). For comparison we also plot the yield of 200 clusters from a deep ROSAT PSPC X-ray cluster survey [9]. Note that after a one month SZE survey we will have more redshift $z > 0.5$ clusters than the deep ROSAT survey. After one year we expect to have ~100 clusters at redshifts $z > 1$ and almost 400 clusters at redshifts $z > 0.5$ [11]. This highly sensitive probe for massive collapsed structures in the high redshift universe constitutes an exceedingly powerful test of current structure formation models.

The SZE survey itself will yield a list of galaxy clusters and constraints on the cluster surface density. Cluster redshifts, masses, gas distributions and galaxy populations can then be examined through followup observations with X-ray satellites and 8 m class telescopes like the VLT. We anticipate that the scope and number of scientific issues addressed with followup observations of the high redshift clusters from the SZE survey will lead to enormous progress in cosmology.

JJM is supported by Chandra Fellowship grant PF8-1003, awarded through the Chandra Science Center. The Chandra Science Center is operated by the Smithsonian Astrophyical Observatory for NASA under contract NAS8-39073. JEC acknowledges support from the David and Lucile Packard Foundation and the James S. McDonnell Foundation.

References

1. Sunyaev, R. A. and Zel'dovich, Y.B., 1972, Comments Astrophys. Space Phys., 4, 173
2. Birkinshaw, M. 1999, *Physics Reports*, 310, num 2-3, 98
3. Carlstrom, J.E., Joy, M.K. & Grego, L. 1996, ApJ, 456, L75
4. Grego, L., Carlstrom, J.E., Joy, M.K., Reese, E.D., Holder, G.P., Patel, S., Cooray, A.R. & Holzapfel, W.L. 1999a, ApJ, submitted
5. Grego, L., Carlstrom, J.E., Joy, M.K., Reese, E.D., Holder, G.P., Patel, S., Cooray, A.R. & Holzapfel, W.L. 1999b, ApJ, submitted
6. Reese, E.D., Mohr, J.J., Carlstrom, J.E., Joy, M.K., Holder, G.P., Patel, S., Grego, L, Holzapfel, W.L., 1999, in preparation
7. Mohr, J.J. & Evrard, A.E. 1997, ApJ, 491, 38
8. Mohr, J.J., Mathiesen, B. & Evrard, A.E. 1999, ApJ, in press, astro-ph/9901281
9. Vikhlinin, A. McNamara, B., Forman, W., Jones, C., Quintana, H., & Hornstrup, A. 1998, ApJ, 502, 558
10. Holder, G.P. & Carlstrom, J.E. 1999, to appear in "Microwave Foregrounds", eds. de Oliveira-Costa & Tegmark (ASP, San Francisco, 1999), astro-ph/9904220
11. Holder, G.P., Carlstrom, J.E. & Mohr, J.J., 1999, in preparation